

Electronic Supporting Information (ESI)

Emulation of Biphasic Plasticity in Retinal Electrical Synapse for Adaptive Pattern Pre-Processing

*Lindong Wu^a, Zongwei Wang^{*a,c}, Bowen Wang^a, Qingyu Chen^a, Lin Bao^a, Zhizhen Yu^a, Yunfan Yang^a,
Yaotian Ling^a, Yabo Qin^a, Kechao Tang^a, Yimao Cai^{*a,b}, and Ru Huang^{*a,b}*

^a Institute of Microelectronics, Peking University, Beijing 100871, P. R. China

^b Frontiers Science Center for Nano-Optoelectronics, Peking University, Beijing 100871, P. R. China

^c Advanced Institute of Information Technology (AIIT), Peking University, Hangzhou, Zhejiang 311215, P. R. China

Email: wangzongwei@pku.edu.cn, caiyimao@pku.edu.cn, ruhuang@pku.edu.cn

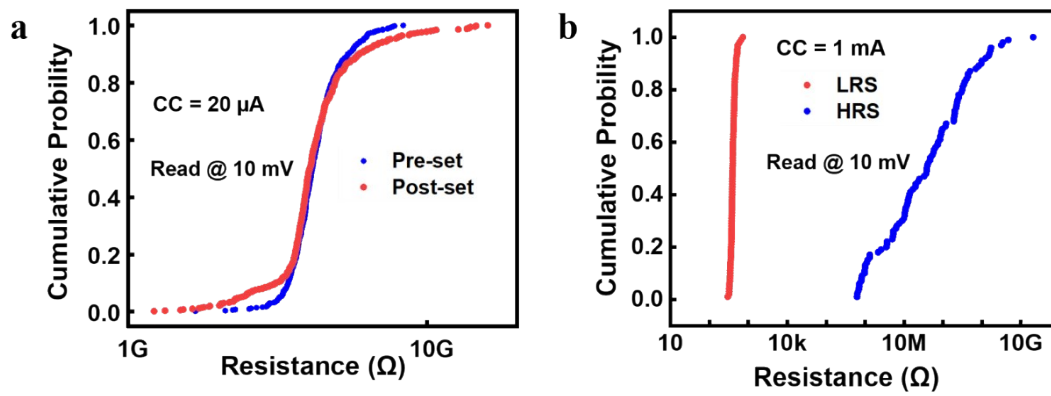


Figure S1. Statistical characteristics of the device under different CCs. (a) The cumulative distributions of pre-set and post-set resistance over the 500 cycles under a 10 mV read voltage when the CC is 20 μA . (b) The cumulative distributions of LRS and HRS for 100 cycles of the device under 10 mV read voltage when the CC is 1 mA. Both distributions show that the device has a good uniformity.

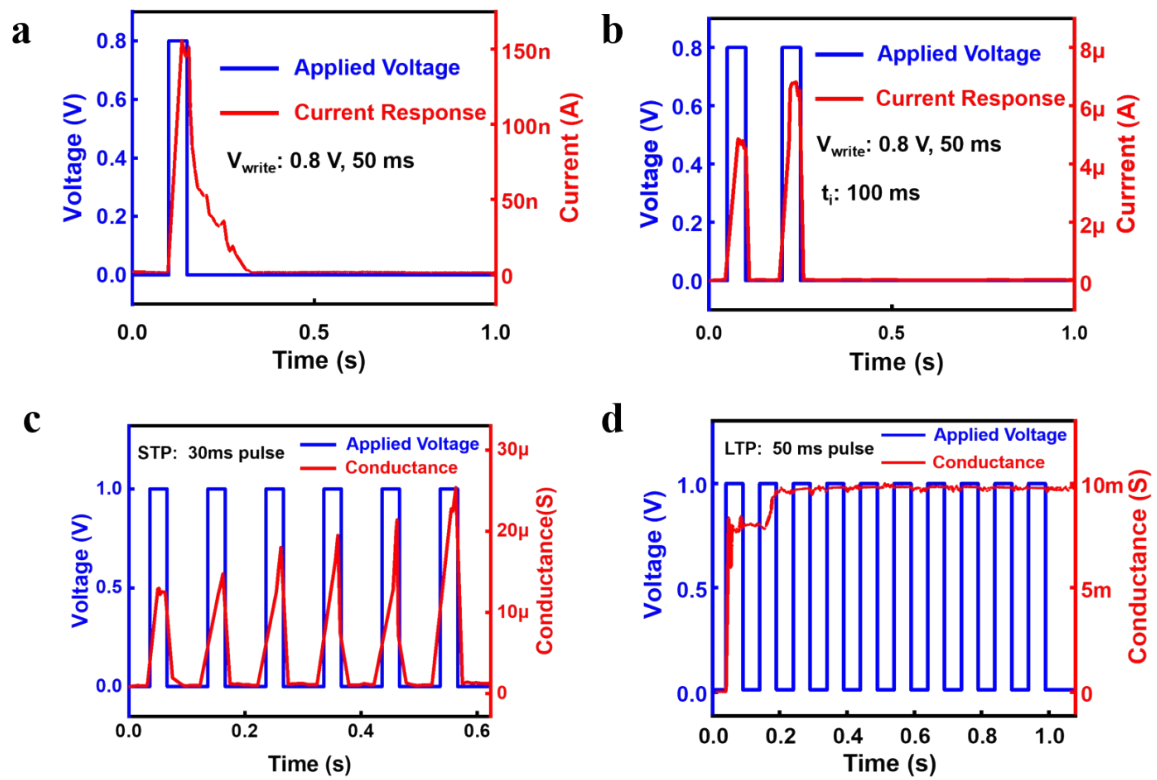


Figure S2. Chemical synaptic plasticity achieved by Ag/SiO₂/Pt device. (a) The EPSC behavior achieved when single weak pulse (0.8 V, 50 ms) is applied. (b) PPF realized by a pair of pulses (0.8 V, 50 ms) with a small interval time ($t_i = 100$ ms). (c) STP behavior observed when 6 consecutive weak pulses (1 V, 30 ms) are applied. During the whole measurement, a constant read voltage of 0.01 V is applied to monitor the conductance change. (d) LTP behavior observed when 10 stronger pulses (1 V, 50 ms) are applied. During the measurement, a read voltage of 0.01 V is applied to monitor the conductance change.

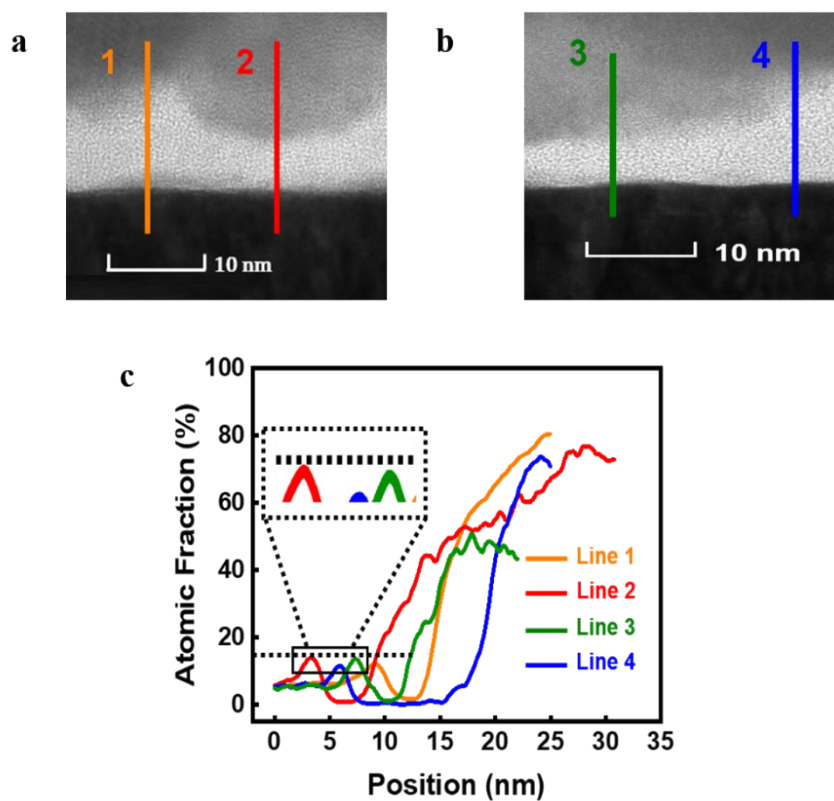


Figure S3. Silver content in different regions. (a-b) Fractured filaments in different devices. (c) Atomic fraction of silver in four regions, including an orange line near filament of device (a), a red line on filament of device (a), a green line on filament of device (b) and a blue line near filament of device (b).

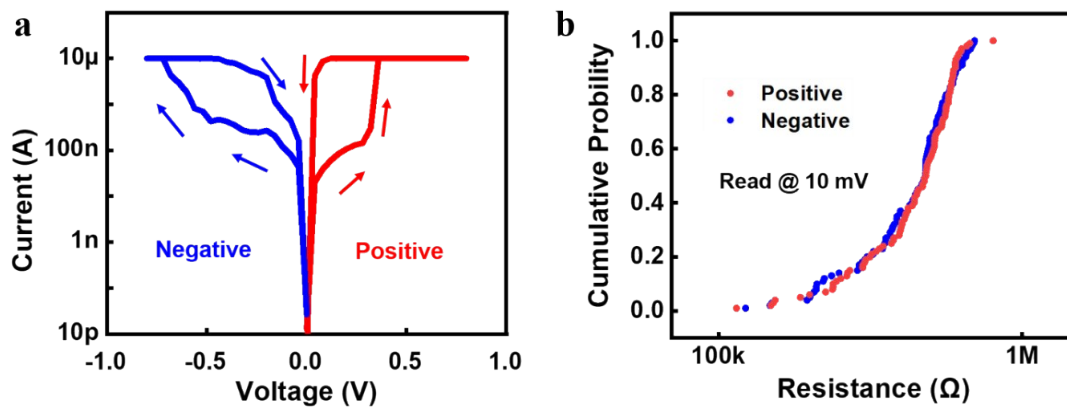


Figure S4. Bidirectional volatile switching characteristic of the Ag/SiO₂/Pt device. (a) Bidirectional volatile switching behavior was observed under 10 μA CC after pretreatment pulse is applied on the device. (b) The cumulative distributions of device resistance read under 10 mV bias over 100 positive set cycles and 100 negative set cycles.

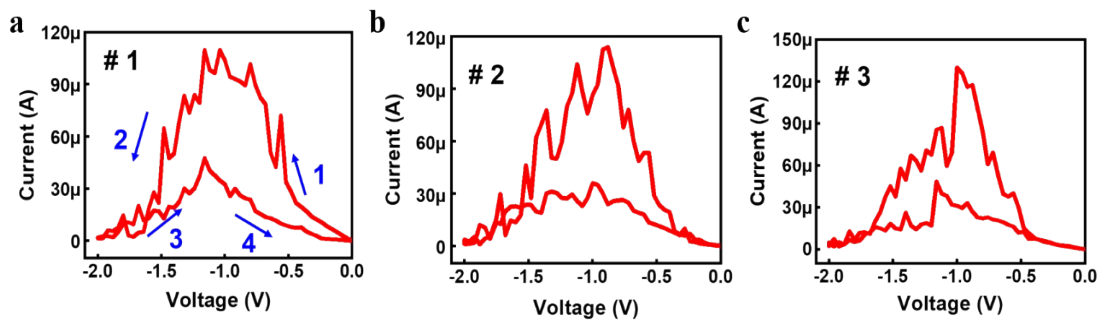


Figure S5. Negative-set behavior under 1 mA CC. (a) The resistance of the device increases first and then decreases when a negative voltage is applied. (b-c) negative-set behaviors are also observed in two other devices.

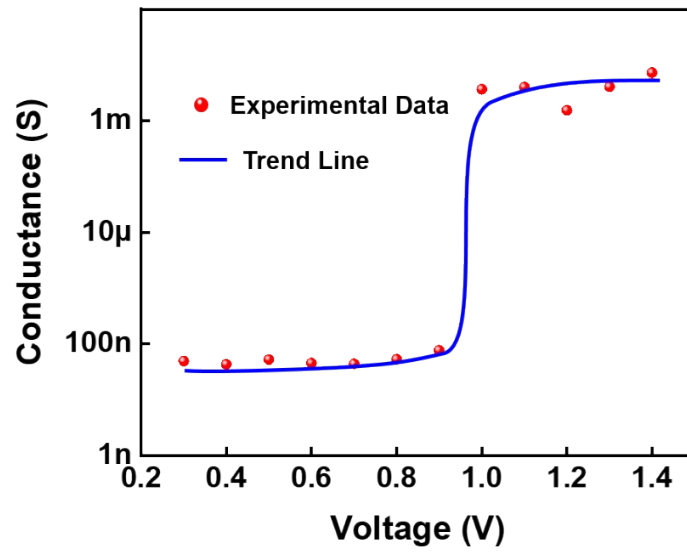


Figure S6: The measurement results of the conductance when a series of (+) pulses with different amplitudes but the same width of 50 ms are applied on the device after the pre-treatment step.

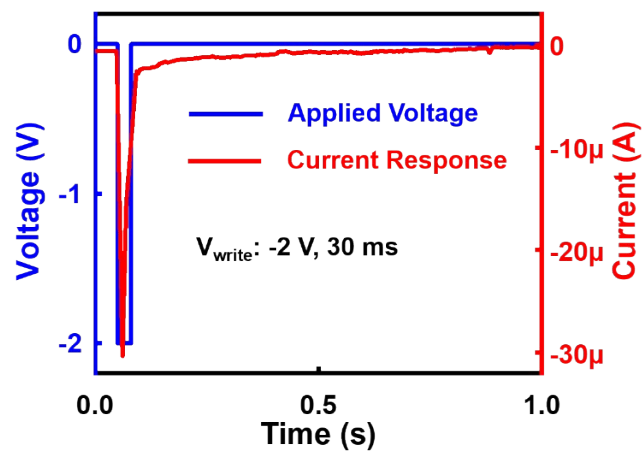


Figure S7: IPSC triggered by a negative pulse (-2 V, 30 ms) after the device was operated by the pretreatment pulse.

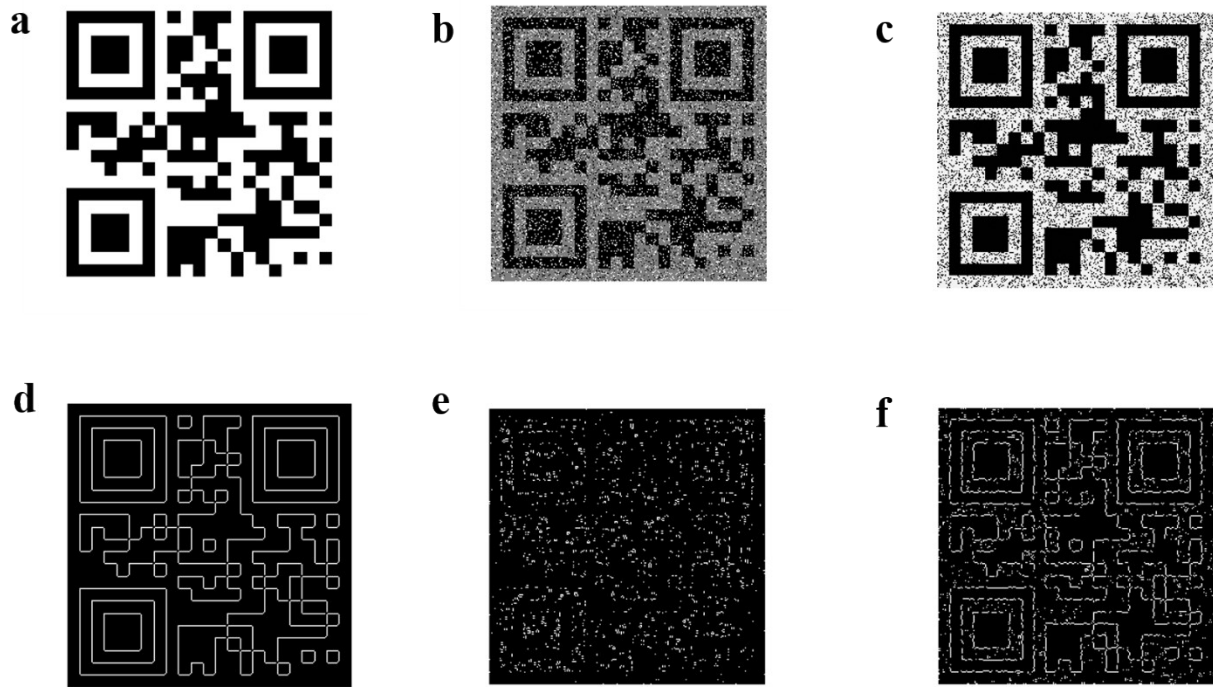


Figure S8. The results of edge extraction of the images under normal illumination (d), noisy dim illumination (e), and noisy dim illumination with pre-processed by OPU array (f). Corresponding images before edge extraction are shown in (a-c).



Figure S9. The simulation results of the images under bright daylight condition. (a) The original QR code image. (b) The image is overexposed under bright daylight condition. (c) The pre-processing result by OPU array proves the contrast enhancement effect.

Demonstration of Dynamic Real-Time Preprocessing Ability by Biphasic Plasticity

We further explored the ability of dynamic real-time preprocessing based on biphasic plasticity with the noise-interfered radar images (Figure S10, Supporting Information). Figure S10(a), Supporting Information is a schematic diagram of radar tracking a plane and transmitting information. The radar first transmits a beam of electromagnetic wave. When encountering an obstacle, the wave will be reflected back to the radar signal receiver, and then radar continuously transmits the electromagnetic wave in a sector to track the detected object. The information the radar receives will all be sent to the processor for analysis. However, when there is a strong noise interference suddenly, the signals will be very distorted, which is simulated by applying salt and pepper noise on a gray image. By inserting a middle layer, namely the array, between signal receiver and processor, the signals will become accurate again. The salt and pepper noise is composed of some black and white pixels represented by 0 and 255 respectively, which will all be set to 0 by the array, reducing much noise. Meanwhile, the pixel values near 128 will be transformed into 255, and the too low or too high pixel values will be set to 0, which greatly promote the contrast. The original image, noisy image, pre-processed image and the contour maps extracted respectively are shown in Figure S10(b-g), Supporting Information.

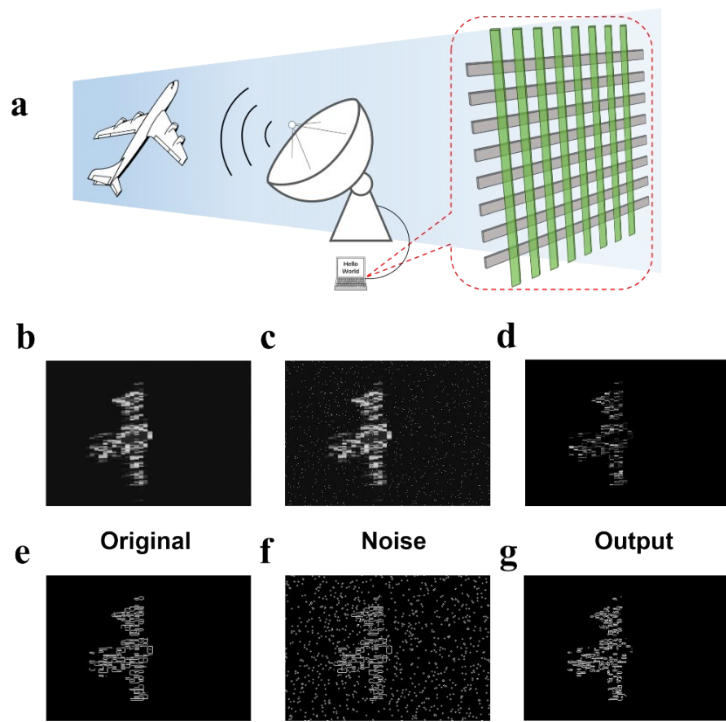


Figure S10. Simulation of adaptive pattern pre-processing with dynamic radar images as an example. (a) Schematic illustration of the whole simulation process. (b) The original radar image. (c) The radar image interfered by salt and pepper noise. (d) The pre-processing result by the array. (e) The corresponding result of edge extraction of original radar image. (f) The edge extraction result of radar image interfered by the noise. (g) The edge extraction result of the image pre-processed by the array. The results of edge extraction confirm that adaptive pre-processing by the array greatly improves the image quality.